

# Magnetic properties of MBE grown $\text{Mn}_4\text{N}$ on MgO, SiC, GaN and $\text{Al}_2\text{O}_3$ substrates

Cite as: AIP Advances 10, 015238 (2020); doi: 10.1063/1.5130485

Presented: 7 November 2019 • Submitted: 23 October 2019 •

Accepted: 19 December 2019 • Published Online: 23 January 2020



Zexuan Zhang,<sup>1,a)</sup> Yongjin Cho,<sup>1</sup> Jashan Singhal,<sup>1</sup> Xiang Li,<sup>1</sup> Phillip Dang,<sup>2</sup>  Hyunjea Lee,<sup>1</sup> Joseph Casamento,<sup>3</sup>  Yongjian Tang,<sup>4</sup>  Huili Grace Xing,<sup>1,3,5</sup>  and Debdeep Jena<sup>1,3,5</sup> 

## AFFILIATIONS

<sup>1</sup>School of Electrical and Computer Engineering, Cornell University, Ithaca, New York 14853, USA

<sup>2</sup>School of Applied and Engineering Physics, Cornell University, Ithaca, New York 14853, USA

<sup>3</sup>Department of Materials Science and Engineering, Cornell University, Ithaca, New York 14853, USA

<sup>4</sup>Laboratory of Atomic and Solid-State Physics, Cornell University, Ithaca, New York 14853, USA

<sup>5</sup>Kavli Institute at Cornell for Nanoscale Science, Cornell University, Ithaca, New York 14853, USA

**Note:** This paper was presented at the 64th Annual Conference on Magnetism and Magnetic Materials.

<sup>a)</sup>Electronic mail: [zz523@cornell.edu](mailto:zz523@cornell.edu)

## ABSTRACT

$\text{Mn}_4\text{N}$  is a compound magnetic material that can be grown using MBE while exhibiting several desirable magnetic properties such as strong perpendicular magnetic anisotropy, low saturation magnetization, large domain size, and record high domain wall velocities. In addition to its potential for spintronic applications exploiting spin orbit torque with epitaxial topological insulator/ferromagnet bilayers, the possibility of integrating  $\text{Mn}_4\text{N}$  seamlessly with the wide bandgap semiconductors GaN and SiC provides a pathway to merge logic, memory and communication components. We report a comparative study of MBE grown  $\text{Mn}_4\text{N}$  thin films on four crystalline substrates: cubic MgO, and hexagonal GaN, SiC and sapphire. Under similar growth conditions, the  $\text{Mn}_4\text{N}$  film is found to grow single crystalline on MgO and SiC, polycrystalline on GaN, and amorphous on sapphire. The magnetic properties vary on the substrates and correlate to the structural properties. Interestingly, the field dependent anomalous Hall resistance of  $\text{Mn}_4\text{N}$  on GaN shows different behavior from other substrates such as a flipped sign of the anomalous Hall resistance.

© 2020 Author(s). All article content, except where otherwise noted, is licensed under a Creative Commons Attribution (CC BY) license (<http://creativecommons.org/licenses/by/4.0/>). <https://doi.org/10.1063/1.5130485>

## I. INTRODUCTION

Epitaxial growth of ferromagnets by molecular beam epitaxy (MBE) is of high technical interest for spintronic applications such as devices exploiting spin orbit torque (SOT). Recently, spin orbit switching in MBE grown ferromagnet/topological insulator bilayers with a critical current as low as  $1.5 \text{ MA/cm}^2$  has been demonstrated.<sup>1</sup>  $\text{Mn}_4\text{N}$ , which is a room temperature ferrimagnet, has been successfully grown by MBE by a few groups.<sup>2-5</sup> These MBE grown  $\text{Mn}_4\text{N}$  films show strong perpendicular magnetic anisotropy ( $K_u = 1.1 \times 10^5 \text{ J/m}^3$ ), low saturation magnetization ( $M_s = 6.6 \times 10^4 \text{ A/m}$ ),<sup>6</sup> large domain size ( $\sim$ millimeter size on STO),<sup>5</sup> and record high domain wall velocities driven by spin transfer torque (up to  $900 \text{ m/s}$ ).<sup>6</sup> This makes  $\text{Mn}_4\text{N}$  attractive for spintronic devices. Meanwhile, the

successful growth of  $\text{Mn}_4\text{N}$  on SiC<sup>4</sup> indicates a strong potential for the seamless integration of  $\text{Mn}_4\text{N}$  with wide bandgap semiconductors of the hexagonal crystal family such as SiC, GaN, AlN, and Sapphire. Such integration may bring spintronic functionality into the burgeoning electronics and photonics applications that these wide-bandgap semiconductor platforms are enabling today.<sup>7</sup>

Most reports on the epitaxial growth of  $\text{Mn}_4\text{N}$  are on oxide substrates such as MgO and  $\text{SrTiO}_3$  (STO). Detailed study of the magnetotransport properties such as the anomalous Hall effect of MBE  $\text{Mn}_4\text{N}$  films grown on other substrates are still lacking. In this work, we report the successful MBE growth of  $\text{Mn}_4\text{N}$  films on four substrates: cubic MgO, and wide bandgap semiconductors (SiC and GaN) and sapphire, the last three of which are hexagonal. A comparative study of the crystalline, structural, electronic, magnetic, and

magnetotransport properties of the  $Mn_4N$  epitaxial films on the four substrates is conducted.

## II. GROWTH AND CHARACTERIZATION METHODS

The  $Mn_4N$  layers were grown by plasma assisted MBE in a Veeco GEN II system. All  $Mn_4N$  films were grown directly on the substrates without any homoepitaxial buffer layer. The growths on all 4 substrates were performed at a thermocouple temperature of 700 °C (unless stated otherwise) for one hour. The growth was monitored by *in situ* reflection-energy electron diffraction (RHEED). A detailed description of sample preparation and characterization methods are provided in the supplementary section.

## III. RESULTS AND DISCUSSIONS

### A. Crystal quality

Manganese nitride is known to crystallize in several bulk phases such as  $MnN$ ,  $Mn_3N_2$ ,  $Mn_2N_x$  and  $Mn_4N$ . Among them, only  $Mn_4N$  is ferrimagnetic.<sup>8</sup> As shown in inset of Fig. 1(a),  $Mn_4N$  has an antiperovskite crystal structure with a nitrogen (N) atom located at the body center, and two inequivalent manganese sites ( $Mn_A$  and  $Mn_B$ ) with magnetic moments of 3.85  $\mu_B$ /f.u. and 0.9  $\mu_B$ /f.u. occupying the corner and face-centered positions,<sup>9</sup> respectively. The crystal structure of  $Mn_4N$  belongs to the space group  $P43m$ , with the  $\{111\}$  planes of  $Mn_4N$  exhibiting trigonal symmetry. Fig. 1(a) shows the energy bandgap and lattice constants of the four substrates chosen in this work. The expected epitaxial relationship of  $Mn_4N$  with the substrates are  $Mn_4N$  (001)//MgO (001) and  $Mn_4N$  (111)//GaN (SiC and sapphire) (0001), as is shown in Fig. 1(b). Among these substrates,  $Mn_4N$  is most lattice and symmetry matched to MgO. The lattice mismatch with sapphire is as high as 74.6%.

Growth of  $Mn_4N$  directly on MgO initiates with a very short nucleation process with spotty RHEED pattern, and gradually changes to bright, streaky pattern as shown in Fig. 2(a) in less than one minute. This indicates a smooth surface, and single crystallinity of the  $Mn_4N$  film. The corresponding X-Ray Diffraction (XRD) spectrum shown in Fig. S1(a) corroborates that the  $Mn_4N$  grown on MgO is single crystal with the 001 orientations out of plane. The additional peak at 40.4 degree might be due to the inclusion of pure Mn or formation of MnO because of oxidation, which has been

reported in previous works.<sup>9,10</sup> The surface is very smooth with root mean square (rms) of 8 angstrom as seen in Fig. S2(a). The structural properties of  $Mn_4N$  grown on MgO are therefore excellent, in line with earlier reports, and its magnetotransport properties are discussed later in a comparative fashion with those grown on the other substrates.

When  $Mn_4N$  is directly grown on GaN, the initial RHEED forms a bright spotty pattern shown in Fig. 2(b). Pairs of symmetric spots on either side of the original first order streaks of  $Mn_4N$  are observed. This RHEED pattern implies the existence of twin domains, that are expected since a three-fold symmetric cubic  $Mn_4N$  crystal is being grown on a six-fold symmetric hexagonal GaN substrate, similar to a recent observation of the growth of cubic ScN on GaN.<sup>11</sup> The RHEED pattern gradually becomes dimmer, and develops into a polycrystalline ring by the end of the one-hour growth as shown in Fig. 2(c). The  $Mn_4N$  thin film deposited directly on GaN is found to be polycrystalline (Fig. S1(b)), evidenced by both (111) and (002) peaks of the crystal. XRD peaks from  $Al_2O_3$  and AlN originate from GaN (on sapphire) templates which were used as substrates for growths in this study.

A strong dependence of the resulting manganese nitride phases on the growth temperature is observed. A secondary phase of  $Mn_2N_{0.86}$  is found to form as evidenced by the XRD peak marked with arrow in the inset of Fig. S1(c), when grown at 600 °C directly on GaN substrates. A possible reason is the thermal stability of the manganese nitride compounds:  $Mn_4N$  is the thermally stable phase at higher temperature than  $Mn_2N_{0.86}$ .<sup>8</sup> The resulting  $Mn_4N$  is rather rough, with a surface rms of 34 nm for a 10x10 micron<sup>2</sup> scan as shown in Fig. S2(b).

For the growth on SiC, the initial RHEED shows a similar spotty pattern during nucleation as seen on GaN (Fig. 2(d)). As can be seen in Fig. S1(d), the epitaxial  $Mn_4N$  on SiC is a single-phase crystal with twinning, showing only the (111) XRD peak, as expected from the symmetry of substrates. The surface morphology is quite rough, characterized by a rms of 38 nm for a 10x10 micron<sup>2</sup> scan as seen in Fig. S2(c). The XRD spectra of single crystalline  $Mn_4N$  is consistent with the spotty RHEED pattern maintained throughout the growth, unlike on the GaN substrate where it becomes polycrystalline.

The MBE growth of  $Mn_4N$  on SiC and GaN with a presumably smoother surface has been reported in Ref. 4. At this stage, we are unable to explain the difference in surface morphology observed earlier and this study. The possible reasons could be different surface treatments or nucleation conditions before growth, or the major difference could stem from the fact that the instead of the plasma source for nitrogen used here, the MBE growths in the previous study was performed using a  $NH_3$  source.<sup>4</sup>

When grown directly on sapphire, the RHEED pattern of manganese nitride develops into very dim and diffusive pattern less than five minutes into the growth. No peaks other than from substrate are seen in the XRD spectrum for the film grown on sapphire, indicating an amorphous nature of the film. From the magnetic characterization shown latter, ferromagnetism is still observed, likely due to nanocrystalline  $Mn_4N$ , the only ferromagnetic phase of manganese nitride at room temperature. The surface morphology is rough with a rms of 66 nm for a 10x10 micron<sup>2</sup> scan as shown in Fig. S2(d). Since the surface of sapphire was not nitridized prior to the deposition, this is likely due to the large lattice mismatch between  $Mn_4N$  and sapphire.

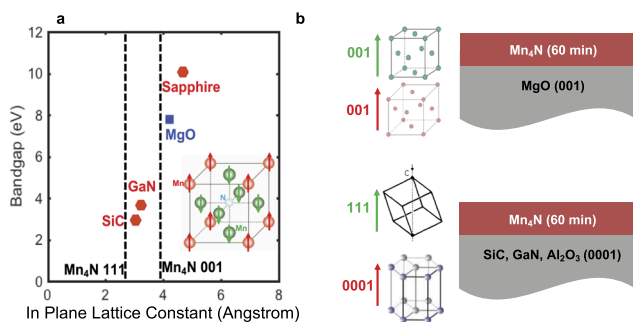


**FIG. 1.** (a) Bandgap and lattice constant of different substrates (inset) Crystal structure of  $Mn_4N$  (b) Schematic of MBE growth of  $Mn_4N$  on different substrates.

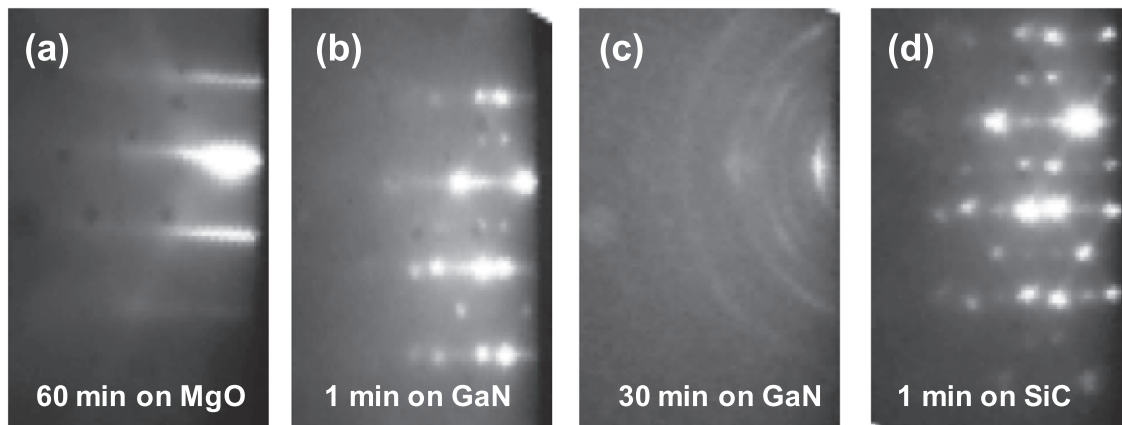


**FIG. 2.** RHEED images (a) 60 min into  $\text{Mn}_4\text{N}$  growth on MgO (b) 1 min into growth on GaN (c) 30 min into  $\text{Mn}_4\text{N}$  growth on GaN (d) 1 min into  $\text{Mn}_4\text{N}$  growth on SiC.

Therefore,  $\text{Mn}_4\text{N}$  grows single crystalline on MgO with smooth surface. On GaN, the  $\text{Mn}_4\text{N}$  film is rough and polycrystalline, with both (002) and (111) orientations out of plane. It is single crystalline on SiC, though the surface is rough. On sapphire, the film is very rough and amorphous. Table S1 summarizes the crystalline qualities of  $\text{Mn}_4\text{N}$  films deposited directly on these substrates without nucleation layers.

## B. Magnetic properties

The film grown on MgO exhibits a square hysteresis loop with almost full remanence at zero field (Fig. 3 (a)). The sharp switching of the magnetization for this sample and comparison with in plane M vs H loop (Fig. S3 (a)) indicate a strong perpendicular magnetic anisotropy (PMA).

The out of plane M vs H loop of  $\text{Mn}_4\text{N}$  on GaN shown in Fig. 3(b) is significantly different from that grown on SiC (Fig. 3(c)). Considering the similarity between SiC and GaN, this sharp contrast

in magnetic properties is quite surprising. Though the saturation magnetization on GaN at 5 K is similar to  $\text{Mn}_4\text{N}$  on SiC, the saturation magnetization drops significantly towards 300 K, reaching only about 50 emu/cc. A similar large drop of the saturation magnetization of  $\text{Mn}_4\text{N}$  with increase in temperature was also reported in  $\text{Mn}_4\text{N}$  grown on  $\text{Pb}(\text{Mg}_{1/3}\text{Nb}_{2/3})\text{O}_3\text{-PbTiO}_3$  (PMN-PT) substrates.<sup>12</sup> It is worth mentioning that magnetic properties of manganese nitride films grown on GaN depend critically on growth temperature, for example there is a large difference in coercive field between the film grown at 700 °C and the film grown at 600 °C with clear evidence of  $\text{Mn}_2\text{N}_{0.86}$  inclusion.

The saturation magnetization and coercive field of  $\text{Mn}_4\text{N}$  on SiC seen in Fig. 3(c) are both comparable to an earlier report.<sup>4</sup> The switching of magnetization is not as sharp as  $\text{Mn}_4\text{N}$  on MgO, possibly due to more structural defects, or weaker PMA on SiC (Fig. S3 (c)). Because strain is believed to be the origin of strong PMA in  $\text{Mn}_4\text{N}$ ,<sup>9,13</sup> the PMA strength is likely to be weaker on strain-relaxed  $\text{Mn}_4\text{N}$  on SiC.

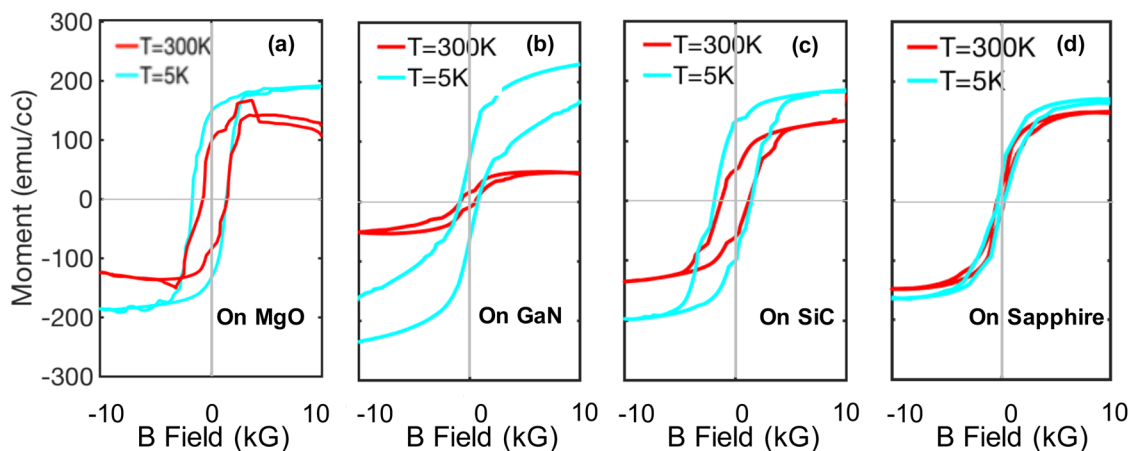


**FIG. 3.** Out of plane M vs H hysteresis curves at 300 K and 5 K of  $\text{Mn}_4\text{N}$  films grown by MBE on (a) MgO (b) GaN (c) SiC and (d) Sapphire.

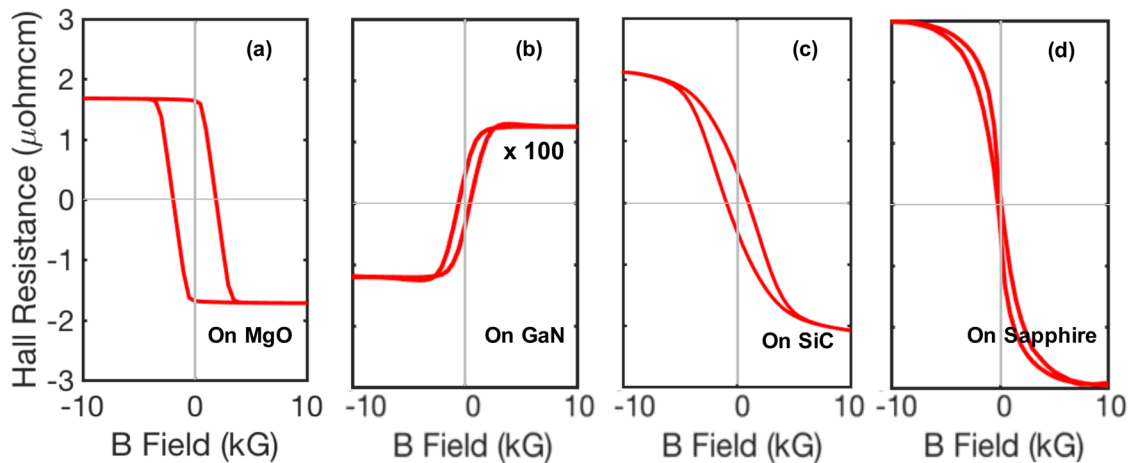


FIG. 4. Anomalous Hall resistance of  $Mn_4N$  grown on (a) MgO (b) GaN (c) SiC and (d) Sapphire at 300K.

Though  $Mn_4N$ -related XRD peaks were not observed for the film grown on sapphire, Fig. 3(d) nevertheless shows a weak hysteresis loop. Since  $Mn_4N$  as the only ferrimagnetic phase at room temperature, it is reasonable to attribute the film grown on sapphire to have  $Mn_4N$  inclusions, though the crystal quality is poor, and the surface is rough.

Comparisons between in plane and out of plane  $M$  vs  $H$  loops of  $Mn_4N$  on different substrates are shown Fig. S3.  $Mn_4N$  epitaxial layers are found to exhibit PMA on all the four substrates.

The longitudinal resistivity  $R_{xx}$  of the  $Mn_4N$  epitaxial layer is  $143 \mu\Omega \text{ cm}$  on MgO, slightly lower than the reported value of  $187 \mu\Omega \text{ cm}$  in Refs. 5 and 6. The longitudinal resistance on GaN is similar to  $Mn_4N$  on MgO. However, layers grown on SiC and sapphire are almost twice as resistive, as summarized in Table. S2. Fig. 4 shows that the anomalous Hall resistance of all the films resemble the shape of the  $M$  vs  $H$  hysteresis curves. However, the Hall resistance is almost two orders smaller for  $Mn_4N$  grown on GaN, than on the other substrates [note the different scales in Fig. 4 (b)]. The Hall angle  $\theta = R_{xy}/R_{xx}$  is as large as 0.01 for  $Mn_4N$  grown on MgO, consistent with earlier reports,<sup>5,6</sup> while being smaller (0.007 and 0.005) when grown on SiC and sapphire respectively. This is the first report on the magneto transport properties of MBE grown  $Mn_4N$  films on substrates other than MgO or STO.

Apart from the extremely small Hall angle (0.002) when grown GaN, the most interesting feature is the sign reversal of the Hall resistance, seen in Fig. 4 and Fig. S4 (a). Such sign reversal of Hall resistance has been reported in other material system such as epitaxial NiCo (002) films<sup>14</sup> and Co/Pd multilayers.<sup>15</sup> However, in these reports, the sign of the anomalous Hall resistance depends on either the thickness of the layer, the temperature, or the composition ratio of multilayers. These are different from the substrate dependence we observe here. The different strain conditions in  $Mn_4N$  films might be a reason, since strain modifies the band structure, resulting in the difference in band filling of  $Mn_4N$  films grown on different substrates.<sup>14</sup> However, it is difficult at this stage to explain the difference between films grown on SiC and GaN considering the similar lattice constant and symmetry of the substrates. On the other hand,

for manganese nitride grown on GaN at lower temperatures, where clear XRD peaks from  $Mn_2N_{0.86}$  can be seen (Fig. S1 (c)), n-type like anomalous Hall resistance is observed (not shown), indicating that the spin states of  $Mn_4N$  can vary significantly due to exchange interaction with other magnetic inclusions such as  $Mn_2N_{0.86}$ .

The sign reversal of anomalous Hall resistance of  $Mn_4N$  film grown on GaN (Fig. S4 (a)) might be a result of the interaction between  $Mn_4N$  and other magnetic inclusions, even though these inclusions are not observed in XRD. This is very likely to happen because of the rich magnetic properties of different phases in (gallium) manganese nitride material system, if we also consider the possibility of inter-diffusion between GaN and  $Mn_4N$ . Furthermore, the observation of the shift in  $M$  vs  $H$  hysteresis loop (Fig. S4 (b)) when field cooling to low temperatures to measure the exchange bias further supports the hypothesis of inclusion of other magnetic phases. Future electron microscopy and chemical analysis is necessary to help unravel the surprising behavior observed in the magnetotransport properties of  $Mn_4N$  grown on GaN. Table. S2 summarizes the measured magnetic properties of the samples in this study.

#### IV. CONCLUSIONS

In summary, ferrimagnetic  $Mn_4N$  films were grown directly on four substrates: MgO, GaN, SiC and sapphire under identical growth conditions. No secondary phases are identified from XRD. Based on RHEED and XRD,  $Mn_4N$  grows single crystalline on MgO and SiC, polycrystalline on GaN, and amorphous on sapphire. The magnetic properties are found to have a strong correlation with the crystal quality.  $Mn_4N$  grown on MgO shows the sharpest switching behavior indicating strong PMA and low density of structural defects. On other substrates, the  $M$  vs  $H$  curves are not as sharp. The anomalous Hall effect shows n-type like behavior when grown on MgO, SiC, and Sapphire. When grown on GaN at a low substrate temperature, the AHE is n-type like behavior, which switches to p-type like behavior when grown at a higher substrate temperature of  $700^\circ \text{C}$ . The sign reversal of the anomalous Hall effect, together with the observation of exchange bias indicates possible inclusion of other

magnetic phases in  $\text{Mn}_4\text{N}$  films grown on GaN. To exploit the integration of  $\text{Mn}_4\text{N}$  with wide bandgap semiconductors such as GaN and SiC by MBE, it is essential that methods of nucleation that lead to much smoother surface morphologies be developed soon. Then, the rich magnetic properties that can already be observed in the current samples can be improved significantly, and the use of epitaxially integrated magnets can enable new applications that take advantage of the wide bandgap semiconductor electronics and photonics platform.

### SUPPLEMENTARY MATERIAL

The [supplementary material](#) provides the details of growth and characterization methods, X-Ray Diffraction (XRD) spectra, atomic force microscopy (AFM) images, additional magnetic characterization data and summary of crystal quality and magnetic properties of  $\text{Mn}_4\text{N}$  films deposited on 4 different substrates.

### ACKNOWLEDGMENTS

This work was supported in part by the Semiconductor Research Corporation (SRC) as nCORE task 2758.001 and NSF

under the E2CDA program (ECCS 1740286) and NewLAW EFRI 1741694. The project used the Shared Facilities sponsored by the NSF MRSEC program (DMR-1719875, CCMR) and MRI DMR-1338010. The authors would also like to thank Prof. Daniel C. Ralph for helpful discussions.

### REFERENCES

- <sup>1</sup>K. N. H. Duy, Y. Ueda, and P. N. Hai, *Nature materials* **17**, 808 (2018).
- <sup>2</sup>Y. Yasutomi *et al.*, *Journal of Applied Physics* **115**, 17A935 (2014).
- <sup>3</sup>M. Meng *et al.*, *Applied Physics Letters* **106**, 032407 (2015).
- <sup>4</sup>S. Dhar, O. Brandt, and K. H. Ploog, *Applied Physics Letters* **86**, 112504 (2005).
- <sup>5</sup>T. Gushi *et al.*, *Japanese Journal of Applied Physics* **57**, 120310 (2018).
- <sup>6</sup>T. Gushi *et al.* arXiv preprint [arXiv:1901.06868](#) (2019).
- <sup>7</sup>D. Jena *et al.*, *Japanese Journal of Applied Physics* **58**, SC0801 (2019).
- <sup>8</sup>K. Suzuki *et al.*, *Journal of alloys and compounds* **306**, 285 (2000).
- <sup>9</sup>Xi Shen *et al.*, *Applied Physics Letters* **105**, 072410 (2014).
- <sup>10</sup>H. Yang *et al.*, *Journal of applied physics* **91**, 1053 (2002).
- <sup>11</sup>J. Casamento *et al.* arXiv preprint [arXiv:1908.01045](#) (2019)
- <sup>12</sup>G. L. Wang *et al.*, *Applied Physics Letters* **113**, 122403 (2018).
- <sup>13</sup>K. Ito *et al.*, *AIP Advances* **6**, 056201 (2016).
- <sup>14</sup>W. J. Fan *et al.*, *J. Phys. D: Appl. Phys.* **48**, 195004 (2015).
- <sup>15</sup>V. Keskin *et al.*, *Applied Physics Letters* **102**, 022416 (2013).